ENVIRONMENTAL RESEARCH
LETTERS

LETTER • OPEN ACCESS

Persistent anomalies of the North Atlantic jet stream and associated surface extremes over Europe

To cite this article: Vera Melinda Galfi and Gabriele Messori 2023 *Environ. Res. Lett.* **18** 024017

ENVIRONMENTAL RESEARCH
LETTERS

LETTER

Persistent anomalies of the North Atlantic jet stream and associated surface extremes over Europe

Vera Melinda Galfi[1,*] and Gabriele Messori[1,2,3,4]

[1] Department of Earth Sciences, Uppsala University, Uppsala, Sweden
[2] Centre of Natural Hazards and Disaster Science (CNDS), Uppsala University, Uppsala, Sweden
[3] Department of Meteorology, Stockholm University, Stockholm, Sweden
[4] Bolin Centre for Climate Research, Stockholm University, Stockholm, Sweden
[*] Author to whom any correspondence should be addressed.

E-mail: vera.melinda.galfi@geo.uu.se

Keywords: jet stream, extreme events, extreme value theory, persistent jet anomalies, large deviation theory

Supplementary material for this article is available online

OPEN ACCESS

RECEIVED
6 September 2022

REVISED
10 December 2022

ACCEPTED FOR PUBLICATION
28 December 2022

PUBLISHED
24 January 2023

Abstract

Unusual, persistent configurations of the North Atlantic jet stream affect the weather and climate over Europe. We focus on winter and on intraseasonal and seasonal time scales, and study persistent jet anomalies through the lens of large deviation theory using Coupled Model Intercomparison Project (CMIP6) simulations of the MPI-ESM-LR model and ERA5 reanalysis data. The configurations of interest are defined as long-lasting anomalies of a few months in jet latitude, speed or zonality. Our results show that persistent temperature and precipitation extremes over large European regions are anomalously frequent during the unusual, persistent jet configurations we identify. Furthermore, the relative increase in frequency of surface extremes is larger for more intense surface extremes and/or more extreme jet anomalies. This is relevant in the context of the predictability of these extremes. The highest extreme event frequencies at the surface are observed in case of precipitation over the Mediterranean and Western Europe during anomalously zonal and/or fast jet events, pointing to these jet anomalies matching rather homogeneous large scale atmospheric configurations with a clear surface footprint. Additionally, our results emphasise the usefulness of large deviation rate functions to estimate the frequency of occurrence of persistent jet anomalies. They therefore provide a tool to statistically describe long-lasting anomalies, much like extreme value theory may be used to investigate shorter-lived extreme events.

1. Introduction

Zonal jets are one of the key components of the global atmospheric circulation. The dynamical maintenance and flow characteristics of the different jet regimes, notably low-latitude 'thermally driven' or subtropical jets and high-latitude 'eddy-driven' or polar-front jets, hold considerable theoretical interest [e.g. 1–6], yet have also a direct societal relevance. Indeed anomalies in the jet stream can be associated with high-impact surface extremes, and reflect both planetary wave activity and synoptic-scale anomalies [e.g. 7, 8].

Here, we focus on the North Atlantic (NA) sector during winter. In this region and season the subtropical and polar-front jets co-exist and are generally well-separated. There are however periods when a single, merged jet may result from the spatial coincidence of thermal and eddy-related jet driving mechanisms [e.g. 9]. Both anomalies in the polar-front jet and merged flow episodes can favour a range of surface extremes in Europe, for example in precipitation, temperature, surface wind or particular matter concentrations [e.g. 8, 10–15]. A parallel stream of literature has focused on linking planetary waves to surface extremes [e.g. 16–19]. While anomalies in the jet do reflect planetary wave activity, we focus here on studies which have explicitly diagnosed anomalies in the jet stream itself.

There are different perspectives in the literature on jet stream variability and its connection to surface weather. Woollings *et al* [20] took a latitude-based approach, identifying preferred meridional locations of the polar-front jet over the NA. These can be linked to different blocking and large-scale

circulation regimes [21, 22], and in turn different weather anomalies in Europe [23]. Woollings *et al* [20] also looked at jet speed, while others have considered jet meandering [e.g. 24], jet tilt [e.g. 9, 25] or distributions of jet axis locations [26]. The dynamical link between the jet stream and surface extremes is often mediated by synoptic systems, such as extratropical cyclones. The jet plays an important role in cyclogenesis and cyclone intensification, and more generally affects the location of storm tracks [27, 28]. This results in a modulation of surface weather, including wind and precipitation extremes [7, 10, 13, 29]. Jet stream anomalies also reflect atmospheric blocking events, which in turn are directly connected to surface temperature extremes [23, 30, 31]. Persistent jet anomalies can thus lead to regional-scale persistent or recurrent surface extremes [e.g. 9–11].

Some of the above studies have considered persistent jet anomalies, but this has mostly been on a case-study basis. [e.g. 9, 10]. Others have explicitly studied persistent characteristics of specific jet regimes, but without making a direct link to the resulting surface extremes [e.g. 32, 33]. Franzke [34] studied the connection between persistent NA jet regimes, defined based on preferred latitudinal positions, and surface wind speed extremes over Europe. Other types of jet anomalies and surface extremes, however, were not considered. Here, we seek to address this knowledge gap by linking unusual and persistent configurations of the NA jet to temperature and precipitation extremes at the surface over Europe. We define 'unusualness' by quantifying jet latitude, speed and zonality, and adopt a rigorous mathematical framework grounded in large deviation theory (LDT) to provide a statistical characterisation of such persistent anomalies. In this study, we rely on long numerical simulations in order to capture very rare persistent jet events, which are not recorded in reanalysis datasets. We compare, where appropriate, the model results with reanalysis data to account for possible model biases.

The standard mathematical framework to study extreme events is provided by extreme value theory (EVT) [35, 36]. Using EVT, one either defines extremes as maximum values over certain time periods (for example one season or year), or selects them as values above a high threshold. When studying persistent extreme events, however, both intensity and duration are relevant. In the EVT framework, information about the event duration is either missing or is rigidly quantified as a mean asymptotic duration (cluster size) of all extreme events [35, 36]. An alternative approach to analyse persistent extremes has been introduced in [37] and successfully applied to study heatwaves and cold spells [37, 38]. This method leverages LDT and investigates persistent extremes based on extreme values of temporal averages. A heatwave, for example, can be analysed using extremes of temperature averages over a few days or weeks. The LDT-based method incorporates the event duration in a flexible way, based on the averaging time. The results can then be extrapolated towards longer averaging times, i.e. longer lasting anomalies, given the convergence to the large deviation limit.

In this study we are interested in return periods of jet anomalies as a function of their duration, rather than focusing on events with a fixed duration. We thus take the perspective of LDT. However, we also compare the results obtained based on LDT with what would be given by EVT. The structure of the paper is as follows. The data and methods are described in section 2. We present our results in section 3, where we study the connection between persistent NA jet anomalies and surface extremes over Europe and, after that, report the return periods of jet anomalies. Our motivation for estimating frequencies of persistent jet anomalies stems from their direct connection to temperature and precipitation extremes over Europe. We thus cover both these topics in section 3. We summarise and discuss our results in section 4.

2. Data and methods

2.1. Data

We use a 1000 year long CMIP6 pre-industrial control run of the MPI-ESM-LR earth system model with a horizontal resolution of 1.9° [39] and ERA5 reanalysis data [40] for the period 1979–2020 with a horizontal resolution of 0.25°. The chosen model is one of the best performing earth system models of its generation [41, 42]. From the model output, we use daily 250 hPa zonal wind, 2 m air temperature, and daily cumulated precipitation. From the reanalysis, we analyse the daily mean of the 6 hourly 250 hPa zonal wind. To ensure comparable results, the reanalysis data is regridded to the resolution of the model. We focus our analysis on an extended boreal winter season: December, January, February and March (DJFM).

2.2. Jet indices

We consider the zonal component of the wind over the NA at 250 hPa: $u(\lambda, \varphi, t)$, where λ is latitude, φ is longitude and t is time. To distil information from this three-dimensional wind field, we use three jet indices: the zonal jet index (ZJI), the jet speed index (JSI) and the jet latitude index (JLI). These indices are adapted from [9, 20], respectively. Negative or positive values of the indices point to unusual states of the jet stream from different perspectives related to its tilt, speed, or meridional location. The ZJI identifies jet configurations with a clear meridional split between the polar-front and subtropical jet streams versus merged jet configurations. The JSI identifies cases when the zonal flow of the jet is faster or slower than normal.

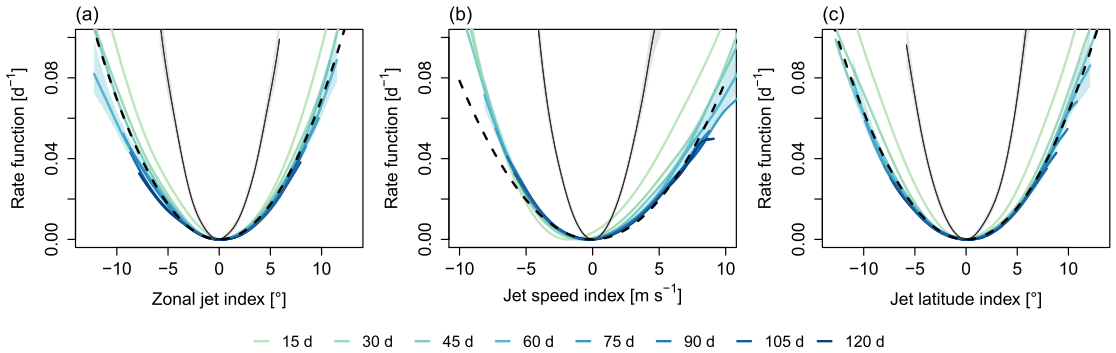

Figure 1. Rate function estimates of the (a) zonal jet, (b) jet speed, and (c) jet latitude indices for increasing averaging times, according to the legend. The blue shading marks bootstrap confidence intervals of the 60 d rate function estimate (1000 replicates), the dashed black line represents the corresponding quadratic fit, and the continuous black line the rate function estimate for randomly shuffled data.

Finally, the JLI shows whether the jet is located further north or further south than usual. To compute the ZJI, we select the region 75° W–50° E and 10°–80° N, whereas for the JSI and the JLI the region 60°–0° W and 15°–75° N is selected. The indices are computed for every day in each dataset as follows.

To obtain the ZJI, we first select at each longitude the latitude of maximum zonal wind, $\hat{\varphi}(\lambda)$. Next, we compute the difference of $\hat{\varphi}$ between neighbouring latitudes and take its maximum absolute value, $\Delta = \max(|\hat{\varphi}(\lambda_i) - \hat{\varphi}(\lambda_{i+1})|)$. The ZJI is the anomaly of Δ relative to its seasonal cycle. We obtain the JSI by selecting the maximum of the zonally averaged zonal wind $U_{\max}$, and computing the anomaly of $U_{\max}$ relative to its seasonal cycle. Taking the latitude $\varphi_{\max}$ corresponding to $U_{\max}$, and then subtracting from $\varphi_{\max}$ its seasonal cycle, gives us the JLI. In case of the model output, we estimate the seasonal cycle based on averaging for each calendar day over all years, whereas in case of the reanalysis, we additionally smooth this seasonal cycle with a 15 d running mean window to reduce the noisiness due to the shorter time series length.

2.3. LDT

We identify persistent configurations of the NA jet stream based on temporal averages of jet indices on intraseasonal and seasonal time scales. We obtain the probability of averaged jet indices—and of the corresponding persistent jet configurations—based on LDT. We consider averages $A_n = \frac{1}{n}\sum_{i=1}^{n} X_i$, where the X_i's are random variables and n is the averaging time. With an increasing averaging time, $n \to \infty$, the probability of averages decays exponentially:

$$p(A_n = a) \approx \mathrm{e}^{-nI(a)}. \tag{1}$$

$I(a)$ is the rate function and quantifies the speed of decay. The rate function is positive almost everywhere, except at the mean of the averages, where it is 0, pointing to the convergence of sample averages to the theoretical mean corresponding to the law of large numbers. In practice, if the averaging time n is large enough and the autocorrelation weak enough, one can approximate the probabilities of averages based on equation (1). To test if this is the case one usually verifies whether the rate function

$$I_n(a) = -\frac{1}{n}\ln p(A_n = a) \tag{2}$$

converges for increasing n. Given the convergence for a certain value n^*, we can then estimate the probabilities for every average over $n \geqslant n^*$ based on the probabilities of averages over n^*.

In case of the considered jet indices, the rate function estimates converge at an averaging block length of approximately 2 months (figure 1). Thus, the rate function estimate for $n = 60$ d can be used to obtain the probability and return periods of averages over a range of averaging times between 60 and 120 d (DJFM season length).

The rate function estimates are approximately quadratic (figure 1), meaning that positive deviations on time scales of 2–4 months are as probable as negative deviations. Furthermore it implies that, from a statistical perspective, large deviations are similar to small deviations around the mean, and can be described by the central limit theorem. In case of Gaussian random variables, the rate function is perfectly quadratic. The rate function of the JSI seems to represent an exception because it deviates slightly from the quadratic fit (figure 1(b)). In section 3 below, we discuss the implications of this anti-symmetry on the return period estimates.

The effect of the autocorrelation on the probabilities of long-lasting jet anomalies becomes visible when comparing the estimated rate functions with the ones obtained based on randomly shuffled data, hence without temporal correlations (figure 1). If we consider, for example, ZJI $= 5°$, the rate function including temporal correlations is $I_1(5) \approx 0.02\,\mathrm{d}^{-1}$, whereas the one without correlations is $I_2(5) \approx 0.08\,\mathrm{d}^{-1}$. The ratio between the two probabilities is obtained using equation (1): $p_1/p_2 = \mathrm{e}^{-n(I_1(5)-I_2(5))}$.

This gives, for $n = 60$ d, a probability ratio of approximately 37. The autocorrelation makes ZJI averages of 5° over 60 d approx. 37 times more probable with respect to uncorrelated data. Figure 1 shows that the autocorrelation in the jet index time series is weak enough in order to allow for the convergence of the rate function estimates, but, at the same time, strong enough to substantially increase the probability of large positive or negative averages.

We quantify the change in probability of surface (2 m air temperature and precipitation) extremes connected to jet events using the ratio between their frequency during jet events and their climatological frequency:

$$r = \frac{f(s > s^* | \mathrm{JI} > \mathrm{JI}^*)}{f(s > s^*)} = \frac{N(s > s^* | \mathrm{JI} > \mathrm{JI}^*)/N(\mathrm{JI} > \mathrm{JI}^*)}{N(s > s^*)/N(s)}, \quad (3)$$

where f is the frequency and N the number of values, s is the considered surface variable and JI the jet index. The thresholds used to identify surface extremes and persistent, unusual jet events are given by s^* and JI*, respectively. Note that equation (3) considers only positive s or JI extremes. Negative extremes, can be selected by taking $s < s^*$ or JI $<$ JI*.

We obtain LDT return period estimates of jet index averages by inverting the probabilities given by equation (1). Similarly, empirical return period estimates are computed by inverting empirical probabilities. To verify the accuracy of the LDT return periods, we compare them with empirical estimates, but also with those obtained by fitting the Generalised Pareto Distribution (GPD) to values above (below) a high (low) threshold. GPD return levels are computed based on the estimated GPD parameters [35].

3. Results

The convergence of rate functions estimates shows that LDT is useful for studying persistent jet anomalies of 2 months and longer. We structure our results around three main topics. First, we compare general jet characteristics and persistent anomalous jet events between the model and reanalysis data. Next, we study the change in frequency of temperature and precipitation extremes over Europe during persistent jet anomalies with respect to climatological conditions. Finally, we obtain return periods of persistent jet anomalies.

3.1. Model representation of jet climatology and variability

We compare jet characteristics between the MPI-ESM-LR model and ERA5 based on the long-term temporal average (climatology) of the 250 hPa zonal wind field, probability density functions (PDFs) of jet indices, and 60 d averages of jet indices (figure 2). The jet climatology in the model is similar to the one in ERA5 (figures 2(a) and (b)), although the mean meridional tilt of the polar-front jet, and thus the split between the polar-front and subtropical jets, is weaker in the model. Despite this discrepancy in the mean state, the PDFs of the zonal jet and jet speed indices correspond closely to the ones from reanalysis data (figures 2(c) and (d)). The correspondence between model and reanalysis is poorer if we consider the JLI. Although the model reproduces the relative maxima found in the reanalysis PDF (figure 2(e)), the modelled jet is too often in its modal position and excursions to the north and south are not as frequent as in the reanalysis data.

Exploring the connection between 60 d averages of the different jet indices, we notice a generally good correspondence between model and ERA5 data (figures 2(f)–(h)). Both show a substantial negative correlation between the ZJI and the JSI (figure 2(g)), suggesting that merged jets are usually anomalously fast, whereas jets that are more split than usual are anomalously slow. The most extreme JSI averages reproduced by the model are not observed in ERA5. The model values range between approximately -8 and 12 m s^{-1}, while the ERA5 values vary between -5 and 5 m s^{-1}. The shorter period of the ERA5 dataset with respect to the model simulations could be a reason for these undersampled extremes. The converse is observed for negative JLI averages: the most extreme event in ERA5 is outside the range of the model, confirming again that the modelled jet is meridionally too bounded.

By comparing the spatial field of the 250 hPa zonal wind between model and reanalysis in case of extreme values of 60 d jet index averages, we find good correspondence between the two datasets, except in case of the JSI (supplement, figures S1(a)–(f)). The correspondence improves a lot if we select events conditioned on both the JSI and the ZJI (figures S1(g) and (h)). This suggests that the discrepancy comes from the undersampling of these events in the reanalysis data (shown also by the lack of green triangles in the upper left corner of figure 2(g)), rather than from the deficiency of the model in simulating the related atmospheric configurations.

Based on the results above, we conclude that the model reproduces most qualitative features of the NA jet variability as observed in reanalysis data, allowing its use to study persistent jet anomalies and their effect on climate extremes in Europe.

3.2. Persistent jet anomalies and persistent climate extremes

In the following, we study the connection between persistent jet anomalies and persistent surface extremes over Europe in MPI-ESM-LR. In agreement with the negative correlation between the ZJI and the JSI, we find opposite links between surface anomalies and these two jet indices. As an example,

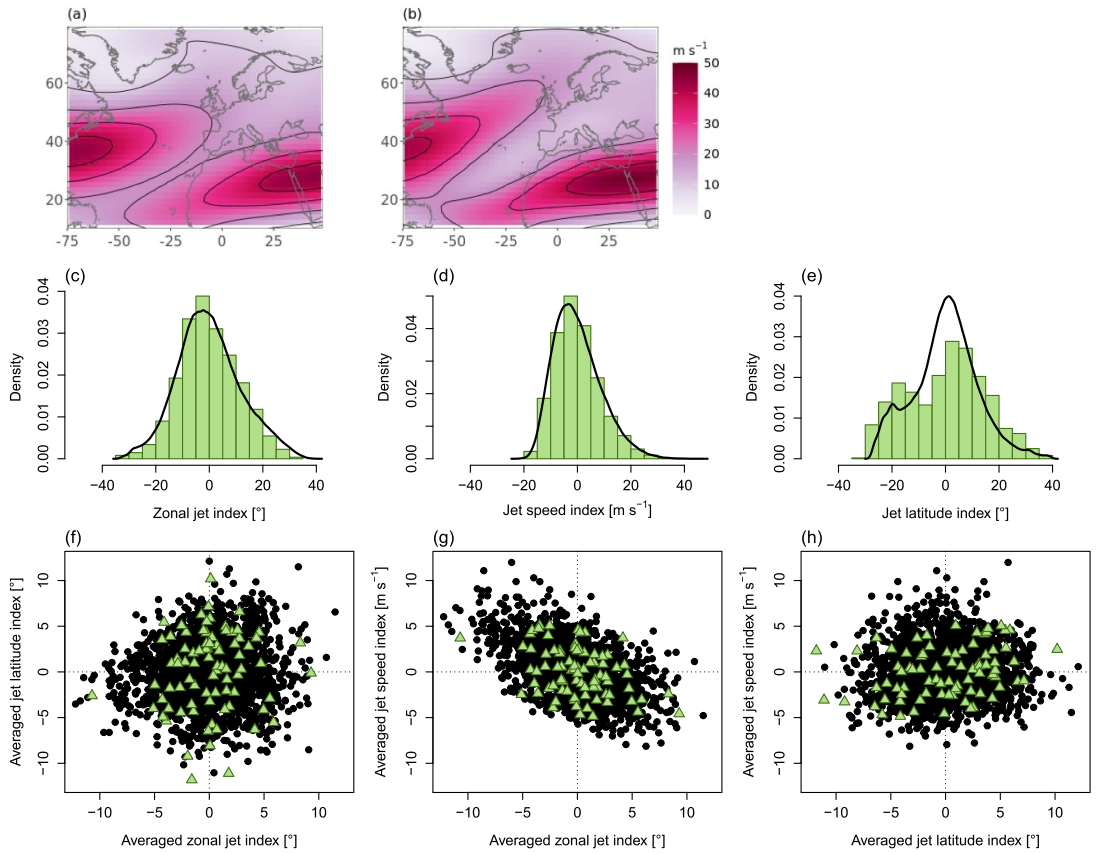

Figure 2. Winter climatology of the zonal wind for (a) the MPI-ESM-LR model and (b) ERA5. Probability density function estimates of (c) the zonal jet index, (d) the jet speed index, and (e) the jet latitude index for model output (black lines) and ERA5 (green bars). Scatter plots of 60 d averages of (f) the zonal jet and jet latitude indices, (g) the zonal jet and jet speed indices, and (h) the jet latitude and jet speed indices, showing both model output (black dots) and ERA5 (green triangles).

an anomalously merged or a faster than usual jet (negative ZJI or positive JSI) is linked to warmer and wetter than usual conditions in the Mediterranean region (figures 3(a), (b), (d) and (e)). In central and northern Europe, large persistent surface anomalies are generally observed during periods with an anomalous JLI and ZJI. When the jet is located more to the north than usual (positive JLI), the region is warmer and wetter than usual (figures 3(c) and (f)). When the jet is anomalously split, we observe similar conditions, albeit shifted northwards (figures 3(a) and (d)). We observe opposite surface effects for jet index anomalies of opposite sign.

Based on figure 3, we qualitatively identify regions where the link between persistent jet configurations and surface anomalies is the strongest (black boxes). The next step is to quantify the change in probability of 2 m air temperature and precipitation extremes connected to jet events in these regions. We focus on persistent surface anomalies, aggregated in time over 60 d (in agreement with the averaging time for jet indices) as well as in space over the regions identified above.

We quantify in figure 4 the relative frequency of persistent temperature and precipitation extremes for increasing intensities of persistent jet anomalies computed based on equation (3). The colours show how many times more frequent temperature or precipitation anomalies become during jet events with respect to their climatological frequency. The temperature and precipitation extremes are defined in terms of averaged values higher (lower) than a range of thresholds, shown on the y-axis in form of quantiles. These are chosen according to figure 3. For example, in case of negative (positive) ZJI extremes we show in figure 4(d) relative frequencies of positive (negative) precipitation extremes over the Western Mediterranean, corresponding to the negative link between the jet index and precipitation extremes in the marked region in figure 3(d). The jet events are defined in an analogous way based on quantiles of averaged jet indices according to the x-axis. The arrows mark the direction of increasing intensities of jet events or surface extremes. Figure 4 leads us to three general conclusions: (a) the relative frequencies are in every case larger than 1, thus surface extremes are more probable during jet events than climatologically; (b) the stronger the jet event, the more frequent are surface extremes; and (c) the connection between jet events and surface extremes increases as we consider stronger surface extremes. The latter point is illustrated by the red and orange colours in

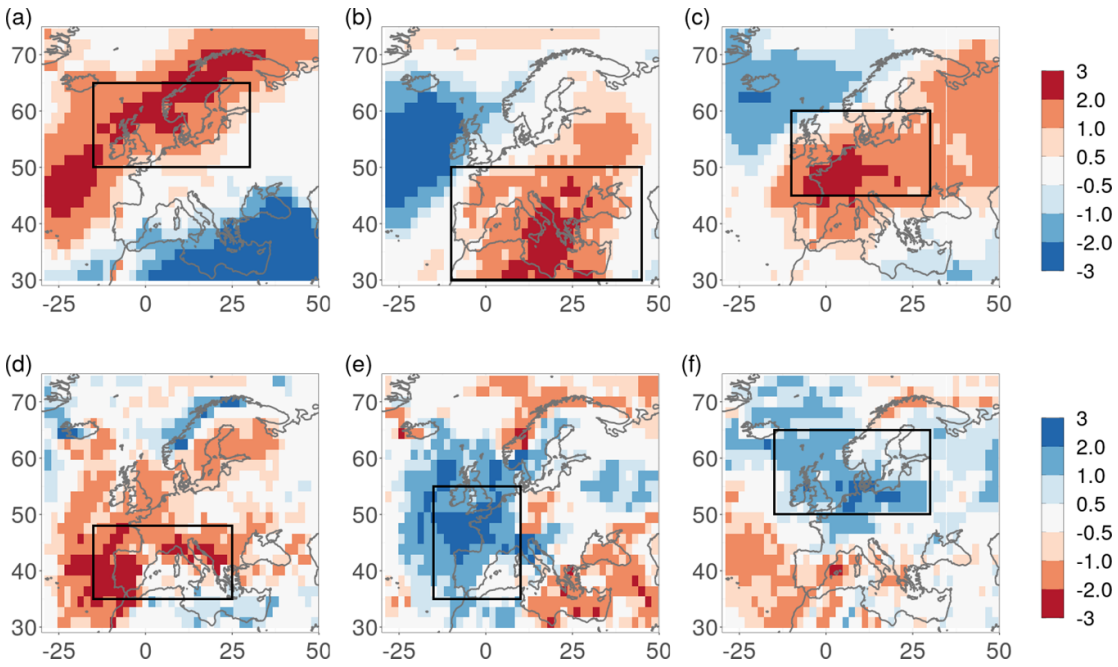

Figure 3. Differences of standardised (a)–(c) temperature and (d)–(f) precipitation anomaly composites in the MPI-ESM-LR model between extreme positive and extreme negative 60 d averages of (a), (d) the zonal jet index, (b), (e) the jet speed index, and (c), (f) the jet latitude index. The standardisation is performed by dividing the 60 d anomaly averages with their standard deviation. The positive (negative) jet index extremes are defined as values larger (lower) than or equal to the 99th (1st) percentile. The black boxes identify regions with strongest temperature or precipitation anomalies.

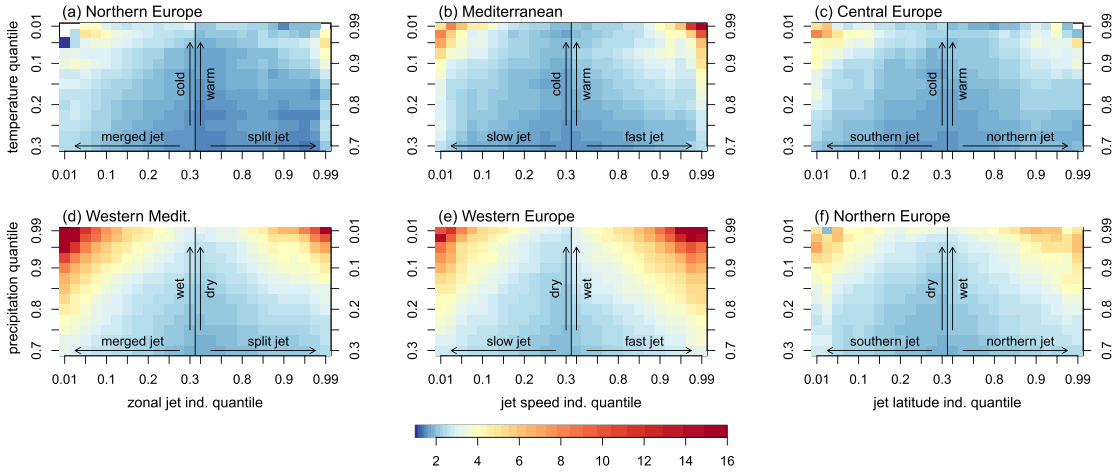

Figure 4. Relative frequencies of persistent (a)–(c) temperature and (d)–(f) precipitation extremes over the regions marked by the black boxes in figure 3 in the MPI-ESM-LR model during persistent anomalies of (a), (d) the zonal jet index, (b), (e) the jet speed index and (c), (f) the jet latitude index, with respect to climatology. All extremes are computed for averages over 60 d and, in case of surface variables, also over the selected regions. Positive (negative) extremes are defined as values above (below) a range of thresholds expressed in terms of quantiles.

the upper left and right corners of the panels, corresponding to extremely negative and positive jet index anomalies, respectively. Whereas the above conclusions are generally true for both temperature and precipitation, the link of jet events with precipitation extremes is much clearer than the one with temperature extremes. The strongest connections are found between anomalously fast or merged jet configurations and positive precipitation extremes (figures 4(e) and (d)).

3.3. Return periods of persistent jet anomalies

We have shown above that persistent jet anomalies increase substantially the frequency of temperature and precipitation extremes over Europe. Thus, it is useful to know how often they occur. We follow the method described in section 2 and obtain return period estimates for positive (negative) averaged jet indices equal or higher (lower) than a range of thresholds, representing the return levels. Due to the predictive power of equation (1), the return periods

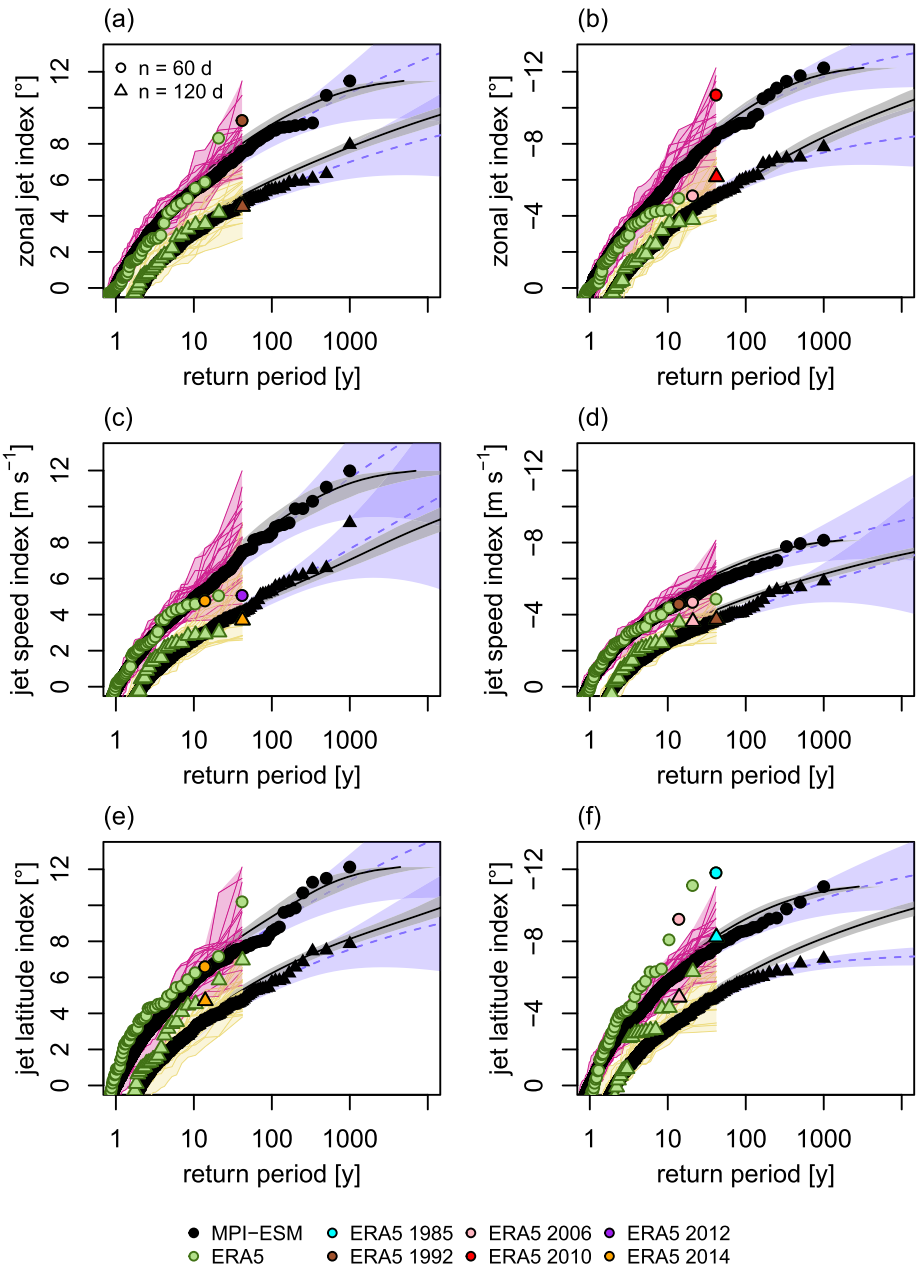

Figure 5. Return levels of positive (left) and negative (right) averages of (a), (b) the zonal jet index, (c), (d) the jet speed index, and (e), (f) the jet latitude index. Black and green markers show empirical estimates based on the MPI-ESM-LR model and ERA5 data, respectively. The black lines represent estimates based on rate functions with 95% bootstrap confidence intervals (gray shading, percentile method). The dashed purple lines show GPD estimates with 95% maximum likelihood confidence intervals (purple shading, we used the functions gpd.fit and gpd.rl of the R package ismev [43]). Circles and triangles show averages over 60 and 120 d, respectively. Other coloured circles (triangles) mark specific winters with unusual weather conditions in the ERA5 data, if the corresponding 60 d (120 d) averages are among the three most extreme recorded values. The magenta (yellow) lines show return levels of 60 d (120 d) averages obtained based on several 41 year chunks of the model data, the corresponding shading highlights the range of these estimates.

of averages over 120 d are obtained based on the rate functions for 60 d averages. Thus, return levels of 120 d averages, reach way beyond empirical estimates (figure 5).

Generally, the LDT return periods correspond very well with the empirical ones and those obtained by fitting a GPD distribution. Because the LDT estimates for 120 d are given by the rate function for 60 d, they are less sensitive to outliers and have a lower uncertainty. We additionally compare the model results with empirical estimates from ERA5. Generally, the correspondence is good (figure 5). However, as expected due to the small sample size in ERA5, we notice some discrepancies for the more extreme values. We test the effect of having shorter time series by taking 41 year chunks of our 1000 years of model output and computing the corresponding return levels. The uncertainty due to the reduced length of the

time series explains the discrepancy between model and reanalysis, except in case of negative JLI extremes (figure 5(f)).

Corresponding to the asymmetric shape of the JSI rate function (figure 1(b)), positive JSI averages are substantially more frequent than negative ones. In case of the other jet indices, the return periods for positive and negative averages are similar.

4. Discussion and conclusions

We have studied the link between wintertime persistent North Atlantic jet anomalies and temperature and precipitation extremes in Europe. We identify the jet anomalies as an unusual tilt, speed, or position of the jet. Using Large Deviation Theory (LDT), we are able to infer the occurrence frequency of unobserved jet anomalies over averaging times $\geqslant$2 and $\leqslant$4 months. We perform the LDT-based analysis on simulations with the MPI-ESM-LR model, and compare the results with the ERA5 reanalysis dataset.

The frequency of persistent temperature and precipitation extremes is systematically increased relative to climatology during persistent jet index extremes. This increase is larger when we consider more anomalous jet configurations, or more extreme surface anomalies. We observe the strongest footprint of persistent jet anomalies when looking at the connection between positive jet speed anomalies and positive precipitation anomalies over the Mediterranean and Western Europe. A strong connection is also observed between anomalously merged jet states and precipitation extremes over roughly the same region, according to the correlation between jet speed and zonality. If the jet is fast, it is conducive to an increased inflow of moist Atlantic airmasses over the continent. Furthermore, a fast jet is usually anomalously merged (figure 2(g)), and directed towards the Mediterranean and Western Europe, favouring cyclonic activity. Thus, anomalously merged jets represent a set of rather homogeneous configurations, with coherent impacts over the identified regions. This confirms previous studies, which showed that a merged jet—linked to the negative phase of the North Atlantic Oscillation [9]—is characterized by a low local dimension and high persistence in the phase space [6, 44]. In line with these results, [45] found that the variability of the jet's latitudinal location decreases with increasing jet speed. On the contrary, a slow jet is related to more heterogeneous configurations.

When comparing the jet index return periods between the model and ERA5, we find that discrepancies for rarely observed values can be explained by the shorter length of the ERA5 dataset, except in case of the jet latitude index. This probably relates to the already discussed deficiency of the model, in which the southern jet states are not frequent and persistent enough.

Our analysis is based on long model simulations with one of the best performing CMIP6 models [41, 42]. We expect that our main conclusions - such as the stronger connection between jet and surface extremes over Europe with increasing intensity of the anomalies, the clearer link between jet events and precipitation extremes compared to temperature extremes, the negative relationship between the jet speed and zonal jet indices (shown by both model and ERA5 data in figure 2(g)) - are robust to the choice of the model. Furthermore, the correspondence between MPI-ESM-LR and ERA5 regarding the regions with the strongest link between persistent jet and surface anomalies is surprisingly good (compare figure 3 with figure S2 in the supplement). Nonetheless, some discrepancies are noticeable corresponding to the discussed difference in the meridional tilt of the jet (figures 2(a) and (b)). Regarding the occurrence frequency of rare persistent jet configurations, future model intercomparison studies would be useful to detect eventual discrepancies among earth system models.

The analysis in this paper leverages LDT. An alternative approach would be to apply Extreme Value Theory (EVT). We have compared return period estimates obtained using LDT and EVT in figure 5. When studying persistent extremes based on averaged variables, two drawbacks of EVT emerge.

(a) EVT has to be applied repeatedly for every averaging time.
(b) The available data amount decreases, thus the uncertainty and bias increase, with increasing averaging time.

By using LDT, the above issues are mitigated due to the possibility to extrapolate towards increasing averaging times, and thus longer events. Here, we obtain the return periods of 120 d jet index averages based on the rate function of 60 d averages. Therefore, these estimates are generally less uncertain than empirical and EVT-estimates (figure 5). Furthermore, they reach beyond empirical values, providing probabilities of unobserved persistent anomalies.

In case of the jet speed index, we find asymmetric rate functions, pointing to more frequent persistent fast jet periods compared to slow jet periods, whereas rate functions of the other jet indices are approximately quadratic. Quadratic rate functions are common in case of temperature averages [37, 46]. Their advantage is that one can obtain the probability of persistent anomalies directly based on the standard deviation and auto correlation of the original (unaveraged) time series, as prescribed by the central limit theorem [37].

LDT offers a new framework for persistent weather and climate events. Previous studies used it to analyse persistent temperature anomalies; here, we apply it on persistent jet anomalies. A future

research avenue would be to understand how 'typical' the persistent jet anomalies are. While the notion of 'typicality' of extremes may seem an oxymoron, it has important consequences for their predictability [37, 38]. LDT could be also applied in a multivariate setting to study compound climate events, or joint anomalies in the jet and selected surface variables.

Here, we find that persistent anomalies of the North Atlantic jet stream lead to a heightened frequency of temperature and precipitation extremes over large European regions. To our knowledge, persistent jet anomalies on intraseasonal and seasonal time scales and their relation to surface extremes over Europe have not been studied systematically in the scientific literature prior to this work. Moreover, due to the long temporal coverage of the used model output (1000 years), we are able to study very rare persistent jet anomalies. Our results show that, despite being rare, these events are highly relevant due to their strong connection to intense, persistent temperature and precipitation anomalies. Thanks to LDT, we are able to robustly estimate their return periods.

Data availability statement

The data that support the findings of this study are available upon reasonable request from the authors. ERA5 data is freely available from the Copernicus Climate Change Service at https://cds.climate.copernicus.eu/cdsapp#!/search?type=dataset, CMIP6 MPI-ESM-LR model output is freely available from nodes of the Earth System Grid Federation, e.g. at https://esgf-data.dkrz.de/search/cmip6-dkrz/.

Acknowledgments

V M Galfi wishes to thank Valerio Lucarini for many discussions on the topic of large deviations and to Jacopo Riboldi and Richard Leading for stimulating conversations about atmospheric circulation anomalies and their effect on weather extremes. V M Galfi acknowledges the support of the Air, Water and Landscape Science research programme at the Department of Earth Sciences, Uppsala University. G Messori acknowledges support from the European Union's H2020 research and innovation programme (ERC Grant No. 948309 (CENÆ)).

ORCID iDs

Vera Melinda Galfi https://orcid.org/0000-0002-8965-0880
Gabriele Messori https://orcid.org/0000-0002-2032-5211

References

[1] Held I M 1975 Momentum transport by quasi-geostrophic eddies *J. Atmos. Sci.* **32** 1494–7
[2] Rhines P B 1975 Waves and turbulence on a beta-plane *J. Fluid Mech.* **69** 417–43
[3] Held I M and Hou A Y 1980 Nonlinear axially symmetric circulations in a nearly inviscid atmosphere *J. Atmos. Sci.* **37** 515–33
[4] Held I M and Larichev V D 1996 A scaling theory for horizontally homogeneous, baroclinically unstable flow on a beta plane *J. Atmos. Sci.* **53** 946–52
[5] Lachmy O and Harnik N 2016 Wave and jet maintenance in different flow regimes *J. Atmos. Sci.* **73** 2465–84
[6] Messori G, Harnik N, Madonna E, Lachmy O and Faranda D 2021 A dynamical systems characterization of atmospheric jet regimes *Earth Syst. Dyn.* **12** 233–51
[7] Röthlisberger M, Pfahl S and Martius O 2016 Regional-scale jet waviness modulates the occurrence of midlatitude weather extremes *Geophys. Res. Lett.* **43** 10989–97
[8] Harnik N, Garfinkel C I and Lachmy O 2016 The influence of jet stream regime on extreme weather events *Dynamics and Predictability of Large-Scale, High-Impact Weather and Climate Events* vol 2 (Cambridge: Cambridge University Press) pp 79–94
[9] Harnik N, Galanti E, Martius O and Adam O 2014 The anomalous merging of the African and North Atlantic jet streams during the Northern Hemisphere winter of 2010 *J. Clim.* **27** 7319–34
[10] Santos Jão A, Woollings T and Pinto J G 2013 Are the winters 2010 and 2012 archetypes exhibiting extreme opposite behavior of the North Atlantic jet stream? *Mon. Weather Rev.* **141** 3626–40
[11] Pinto J G, Gómara Iñigo, Masato G, Dacre H F, Woollings T and Caballero R 2014 Large-scale dynamics associated with clustering of extratropical cyclones affecting Western Europe *J. Geophys. Res. Atmos.* **119** 13704–19
[12] Raveh-Rubin S and Wernli H 2015 Large-scale wind and precipitation extremes in the Mediterranean: a climatological analysis for 1979–2012 *Q. J. R. Meteorol. Soc.* **141** 2404–17
[13] Messori G, Caballero R and Gaetani M 2016 On cold spells in North America and storminess in Western Europe *Geophys. Res. Lett.* **43** 6620–8
[14] Messori G, Van Wees D, Pausata F S R, Navarro J C A, Hannachi A and Dentener F J 2018 The impact of future atmospheric circulation changes over the Euro-Atlantic sector on urban $PM_{2.5}$ concentrations *Tellus* B **70** 1–22
[15] Ordóñez C, Barriopedro D and García-Herrera R 2019 Role of the position of the North Atlantic jet in the variability and odds of extreme PM_{10} in Europe *Atmos. Environ.* **210** 35–46
[16] Hanley J and Caballero R 2012 The role of large-scale atmospheric flow and Rossby wave breaking in the evolution of extreme windstorms over Europe *Geophys. Res. Lett.* **39** 21
[17] Screen J A and Simmonds I 2014 Amplified mid-latitude planetary waves favour particular regional weather extremes *Nat. Clim. Change* **4** 704–9
[18] Wolf G, Brayshaw D J, Klingaman N P and Czaja A 2018 Quasi-stationary waves and their impact on European weather and extreme events *Q. J. R. Meteorol. Soc.* **144** 2431–48
[19] Röthlisberger M, Frossard L, Bosart L F, Keyser D and Martius O 2019 Recurrent synoptic-scale Rossby wave patterns and their effect on the persistence of cold and hot spells *J. Clim.* **32** 3207–26
[20] Woollings T, Hannachi A and Hoskins B 2010 Variability of the North Atlantic eddy-driven jet stream *Q. J. R. Meteorol. Soc.* **136** 856–68
[21] Davini P, Cagnazzo C, Fogli P G, Manzini E, Gualdi S and Navarra A 2014 European blocking and Atlantic jet stream variability in the NCEP/NCAR reanalysis and the CMCC-CMS climate model *Clim. Dyn.* **43** 71–85

[22] Madonna E, Li C, Grams C M and Woollings T 2017 The link between eddy-driven jet variability and weather regimes in the North Atlantic–European sector *Q. J. R. Meteorol. Soc.* **143** 2960–72
[23] Mahlstein I, Martius O, Chevalier Clement and Ginsbourger D 2012 Changes in the odds of extreme events in the atlantic basin depending on the position of the extratropical jet *Geophys. Res. Lett.* **39** L22805
[24] Cattiaux J, Peings Y, Saint-Martin D, Trou-Kechout N and Vavrus S J 2016 Sinuosity of midlatitude atmospheric flow in a warming world *Geophys. Res. Lett.* **43** 8259–68
[25] Messori G and Caballero R 2015 On double Rossby wave breaking in the North Atlantic *J. Geophys. Res. Atmos.* **120** 11129–50
[26] Spensberger C, Spengler T and Li C 2017 Upper-tropospheric jet axis detection and application to the boreal winter 2013/14 *Mon. Weather Rev.* **145** 2363–74
[27] Holton J R 2004 An introduction to dynamic meteorology *International Geophysics Series* 4th edn (Burlington, MA: Elsevier Academic)
[28] Pinto J G, Zacharias S, Fink A H, Leckebusch G C and Ulbrich U 2009 Factors contributing to the development of extreme North Atlantic cyclones and their relationship with the NAO *Clim. Dyn.* **32** 711–37
[29] Leeding R, Riboldi J and Messori G 2023 On Pan-Atlantic cold, wet and windy compound extremes *Weather Clim. Extremes* **39** 100524
[30] Sillmann J and Croci-Maspoli M 2009 Present and future atmospheric blocking and its impact on European mean and extreme climate *Geophys. Res. Lett.* **36** L10702
[31] Masato G, Hoskins B J and Woollings T J 2012 Wave-breaking characteristics of midlatitude blocking *Q. J. R. Meteorol. Soc.* **138** 1285–96
[32] Franzke C, Woollings T and Martius O 2011 Persistent circulation regimes and preferred regime transitions in the North Atlantic *J. Atmos. Sci.* **68** 2809–25
[33] Franzke C and Woollings T 2011 On the persistence and predictability properties of North Atlantic climate variability *J. Clim.* **24** 466–72
[34] Franzke C L E 2013 Persistent regimes and extreme events of the North Atlantic atmospheric circulation *Phil. Trans. R. Soc.* A **371** 20110471
[35] Coles S 2001 An introduction to statistical modeling of extreme values *Springer Series in Statistics* (London: Springer)
[36] Beirlant J, Goegebeur Y, Segers J J J and Teugels J 2004 *Statistics of Extremes: Theory and Applications* (New York: Wiley)
[37] Galfi V M and Lucarini V 2021 Fingerprinting heatwaves and cold spells and assessing their response to climate change using large deviation theory *Phys. Rev. Lett.* **127** 58701
[38] Gálfi V M, Lucarini V, Ragone F and Wouters J 2021 Applications of large deviation theory in geophysical fluid dynamics and climate science *Riv. Nuovo Cimento* **44** 291–363
[39] Mauritsen T *et al* 2019 Developments in the MPI-M Earth system model version 1.2 (MPI-ESM1.2) and its response to increasing CO_2 *J. Adv. Model. Earth Syst.* **11** 998–1038
[40] Hersbach H *et al* 2020 The ERA5 global reanalysis *Q. J. R. Meteorol. Soc.* **146** 1999–2049
[41] Eyring V, Bony S, Meehl G A, Senior C A, Stevens B, Stouffer R J and Taylor K E 2016 Overview of the Coupled Model Intercomparison Project Phase 6 (CMIP6) experimental design and organization *Geosci. Model Dev.* **9** 10539–83
[42] Bock L, Lauer A, Schlund M, Barreiro M, Bellouin N, Jones C, Meehl G A, Predoi V, Roberts M J and Eyring V 2020 Quantifying progress across different CMIP phases with the ESMValTool *J. Geophys. Res. Atmos.* **125** e2019JD032321
[43] Original S functions written by Janet E Heffernan with R port and R documentation provided by Alec G Stephenson 2018 ISMEV: An Introduction to Statistical Modeling of Extreme Values R package version 1.42
[44] Faranda D, Messori G and Yiou P 2017 Dynamical proxies of North Atlantic predictability and extremes *Sci. Rep.* **7** 1–10
[45] Woollings T *et al* 2018 Daily to decadal modulation of jet variability *J. Clim.* **31** 1297–314
[46] Gálfi V M, Lucarini V and Wouters J 2019 A large deviation theory-based analysis of heat waves and cold spells in a simplified model of the general circulation of the atmosphere *J. Stat. Mech. Theory Exp.* **2019** 033404